Seismic wavespeed images across the Iapetus and Tornquist suture zones

Hejun Zhu,[1] Ebru Bozdağ,[1] Daniel Peter,[1] and Jeroen Tromp[1,2]

Received 9 July 2012; revised 9 August 2012; accepted 15 August 2012; published 22 September 2012.

[1] Closures of the Iapetus Ocean and the Tornquist Sea lead to the collision of the paleocontinents of Laurentia, Baltica and Eastern Avalonia during the Caledonian orogeny. It has been speculated that relicts of these two closures may be preserved within the crust or upper mantle. Over the past decades, numerous wide-angle seismic profiles were gathered in northwestern Europe to search for related subsurface features. Although active source studies revealed detailed crustal structures across the Iapetus and Tornquist suture zones, there are relatively few clear three-dimensional upper mantle images beneath this region. We use a new European crust and upper mantle model, EU_{30}, determined based on continental scale, nonlinear adjoint tomography, to explore upper mantle structures across these two suture zones. Model EU_{30} reveals two fast anomalies within the upper mantle: one dips in a northwesterly direction down to approximately 400 km beneath the North Sea, and the other dips in a southwesterly direction down to nearly 250 km across the Tornquist Suture Zone. In addition, we observe a "gap" between the lithospheres of Laurentia and Eastern Avalonia across the Iapetus Suture Zone beneath the central British Isles. These seismic images suggest that heterogeneity related to the closures of the Iapetus Ocean and the Tornquist Sea have been preserved within the upper mantle over hundreds of millions of years. **Citation:** Zhu, H., E. Bozdağ, D. Peter, and J. Tromp (2012), Seismic wavespeed images across the Iapetus and Tornquist suture zones, *Geophys. Res. Lett.*, *39*, L18304, doi:10.1029/2012GL053053.

1. Introduction

[2] During the Neoproterozoic and Paleozoic eras (~600–400 Ma), the Iapetus Ocean — regarded as a predecessor of the Atlantic Ocean — was a relatively wide ocean separating three paleocontinents, namely Laurentia, Baltica and Eastern Avalonia [*Abramovitz et al.*, 1999]. Between Baltica and Eastern Avalonia there was a relatively narrow waterway named the Tornquist Sea [*Cocks and Fortey*, 1982]. These three paleocontinents collided during the Caledonian orogeny (~440 Ma) and formed Laurussia. This collision lead to the closures of the Iapetus Ocean and the Tornquist Sea, and resulted in the Iapetus Suture Zone (ISZ) and the Tornquist Suture Zone (TSZ) [*Abramovitz et al.*, 1999]. In northwestern Europe, the ISZ has been identified beneath Ireland, the British Isles, and the North Sea. The TSZ, which is also known as the Trans-European Suture Zone, has mainly been found beneath northern Germany and southern Scandinavia, consisting of the Sorgenfrei-Tornquist Zone in the northwest and the Teisseyre-Tornquist Zone in the southeast [*Shomali et al.*, 2002, 2006] (see Figure 1).

[3] Numerous wide-angle active source experiments were designed to investigate seismic structures beneath these two ancient suture zones, such as CSSP [*Bott et al.*, 1985], BIRPS [*Klemperer and Matthews*, 1987], VARNET-96 [*Landes et al.*, 2000], MONA LISA [*Abramovitz et al.*, 1998, 1999; *Abramovitz and Thybo*, 2000; *Lyngsie and Thybo*, 2007], and the TOR array [*Arlitt et al.*, 1999; *Shomali et al.*, 2002; *Gregersen et al.*, 2002; *Shomali et al.*, 2006]. Using reflection data from the BIRPS experiment, *Klemperer and Matthews* [1987] found prominent crustal reflectors dipping in a NNW direction across the ISZ beneath the central British Isles. The VARNET-96 and MONA LISA profiles were used to identify significant differences in crustal structure across the ISZ beneath Ireland, as well as across the TSZ beneath the eastern North Sea [*Abramovitz et al.*, 1998, 1999; *Abramovitz and Thybo*, 2000]. Based on a S waveform inversion, *Zielhuis and Nolet* [1994a] found a strong upper mantle contrast in shear wavespeed across the TSZ, which is difficult to observe from previous active source experiments. *Shomali et al.* [2002, 2006] used teleseismic body-wave tomography based on TOR array data to investigate 2D P and S wavespeed structures across the TSZ down to nearly 300 km depth. Their model reveals a sharp increase in lithospheric thickness from northern Germany to southern Sweden. They also found a fast wavespeed body dipping in a southwesterly direction and extending down to approximately 200 km beneath northern Germany. The location of this fast wavespeed body coincides with the surface expression of the Elbe Lineament. *Medhus et al.* [2012] integrated several seismic datasets recorded in northwestern Europe to image upper mantle structure beneath the TSZ and southern Scandinavia. This traveltime tomographic study provided the first targeted upper mantle image beneath this area. However, their vertical resolution is insufficient to reveal detailed structures.

[4] Over the past decade, numerous traveltime tomographic images of the European continent have been produced [e.g., *Bijwaard and Spakman*, 2000; *Piromallo and Morelli*, 2003; *Lebedev and van der Hilst*, 2008]. However, to date, there have been relatively few studies focused on 3D upper mantle images across the ISZ and TSZ. Previous seismic studies were unable to provide such images either because they mainly focused on crustal structure based on active source experiments, or because they were

[1]Department of Geosciences, Princeton University, Princeton, New Jersey, USA.
[2]Program in Applied and Computational Mathematics, Princeton University, Princeton, New Jersey, USA.

Corresponding author: H. Zhu, Department of Geosciences, Princeton University, Guyot Hall 312, Princeton, NJ 08544, USA. (hejunzhu@princeton.edu)

0094-8276/12/2012GL053053

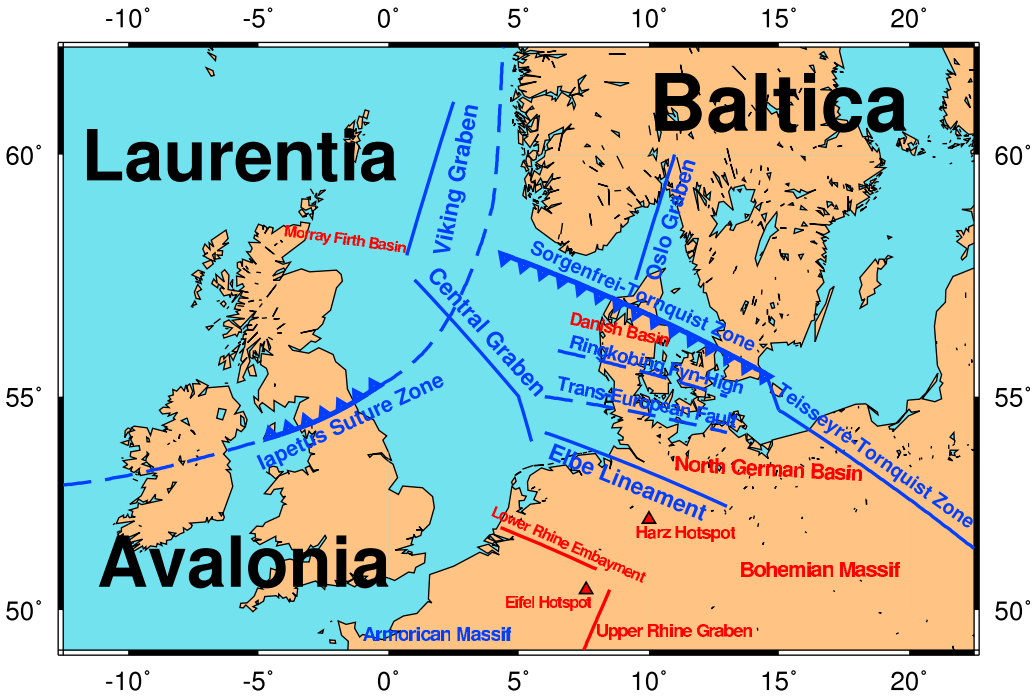

Figure 1. Schematic map of the main tectonic structures in northwestern Europe.

only able to resolve 2D cross sections beneath a local, linear array.

[5] Here, we explore upper mantle structures beneath the ISZ and the TSZ based on a new 3D European crust and upper mantle model, called EU_{30}, derived based on a nonlinear iterative inversion [*Zhu et al.*, 2012]. Several horizontal and vertical cross sections of relative perturbations in vertically propagating and horizontally polarized shear wavespeed, $\delta \ln \beta_v$, are used to investigate upper mantle structure associated with the closures of the Iapetus Ocean and the Tornquist Sea.

2. Data and Method

[6] EU_{30} is a new European crust and upper mantle model derived from continental-scale adjoint tomography [*Zhu et al.*, 2012]. Data from 190 earthquakes recorded by 745 seismographic stations were employed in this study. Three-component seismograms were fully exploited in the inversion, resulting in 26,581 useable seismograms and more than 123,205 frequency-dependent traveltime measurements. In the inversion, short-period body waves and long-period surface waves are combined to constrain seismic structures.

[7] Adjoint tomography is an iterative tomographic procedure which utilizes 3D forward simulations and gradient calculations [*Tromp et al.*, 2005; *Tape et al.*, 2007]. Its benefits include: accurate calculation of synthetic seismograms in fully 3D models, numerical computation of Fréchet derivatives in 3D models, incorporation of finite-frequency effects [*Dahlen et al.*, 2000; *Hung et al.*, 2000], avoidance of "crustal corrections" for imaging the mantle, and full exploitation of three-component seismograms. In the inversion, a spectral-element method [*Komatitsch and Tromp*, 1999, 2002a, 2002b] is used to compute 3D synthetic seismograms, and an adjoint method [*Tarantola*, 1984; *Tromp et al.*, 2005; *Liu and Tromp*, 2006, 2008] is used to calculate 3D misfit gradients. Based on a preconditioned conjugate gradient method [*Fletcher and Reeves*, 1964], we are able to iteratively update the model and progressively minimize discrepancies between observed and simulated seismograms. Adjoint tomography has been successively used to image crustal structure in southern California [*Tape et al.*, 2009, 2010], upper mantle structure beneath Australia [*Fichtner et al.*, 2009, 2010], and crust and upper mantle structure beneath Europe [*Zhu et al.*, 2012]. In this article, we focus on 3D structures across the ISZ and TSZ in new European upper mantle model EU_{30}.

3. The 3D Shear Wavespeed Structure

[8] In Figure 2, we present relative perturbations in β_v for model EU_{30} at various depths, ranging from 75 km to 325 km. Spherically symmetric Earth model STW105 [*Kustowski et al.*, 2008] is chosen as the reference model to calculate the relative perturbations. The Sorgenfrei-Tornquist Suture Zone and the Teisseyre-Tornquist Suture Zone [*Shomali et al.*, 2002, 2006] comprise a striking tectonic feature which separates the Precambrian East European Craton and Phanerozoic central and western Europe [*Zielhuis and Nolet*, 1994a, 1994b; *Artemieva et al.*, 2006]. In EU_{30}, this prominent contrast extends from 75 km down to nearly 250 km. Beneath southern Scandinavia, in the depth range from 75 km to 225 km, we detect a sharp transition between fast and slow anomalies, which was previously discovered by *Medhus et al.* [2012]. The Danish Basin and Northern German Basin are separated by a linear fast anomaly from 75 km to 225 km. At 75 km depth, there are several small-scale features beneath central and western Europe, such as a fast anomaly associated with the Armorican Massif, and slow anomalies related to the Eifel and Harz hotspots, the Bohemian Massif, and the Central Slovakia Volcanic Fields.

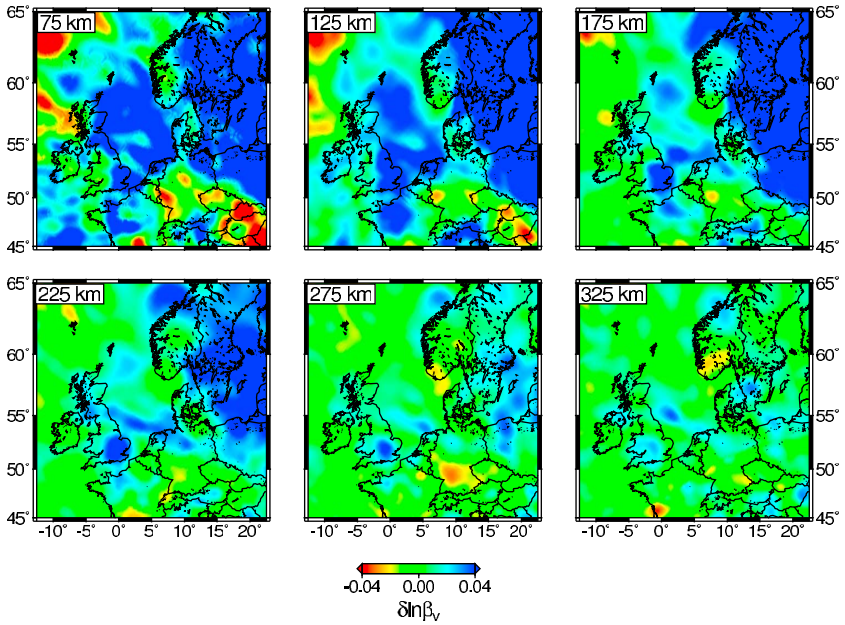

Figure 2. Relative perturbations in the wavespeed of vertically propagating and horizontally polarized shear waves, $\delta \ln \beta_v$, for model EU_{30} at various depths ranging from 75 km to 325 km. Spherically symmetric model STW105 [*Kustowski et al.*, 2008] is used as a reference model. Blue and red colors denote fast and slow wavespeed anomalies, respectively.

[9] Beneath the North Sea, model EU_{30} contains a strong fast anomaly down to depths of nearly 175 km. This fast and presumably cold anomaly may be the cause of the Central Graben. The absence of fast anomalies beneath southwestern Norway and Denmark at depths ranging from 75 km to 225 km may explain their elevated expression. Around 60°N and between 0°E and 5°E, we observe a fast anomaly at depths between 175 km and 225 km, which we interpret as a subsurface structure related to the Viking Graben. At 75 km depth around 58°N and between 7.5°E and 10°E, there is an elongated fast anomaly connecting fast anomalies beneath the North Sea and the Baltic Shield. This structure coincides with the locations of the Skagerrak and Oslo grabens. A relatively small and weak slow anomaly is found beneath the southern coast of Norway between depths of 275 km and 325 km, which may be a result of the rift of the Oslo Graben [*Heeremans et al.*, 1996]. In addition, an interesting NW-SE trending fast anomaly, extending from northern England towards northern Germany, is revealed in the depth range from 175 km down to nearly 325 km. We interpret this feature as the subsurface expression of the Elbe lineament [*Shomali et al.*, 2002, 2006; *Lyngsie et al.*, 2006; *Lyngsie and Thybo*, 2007].

[10] In Figure 3, three vertical cross sections are used to further illustrate upper mantle structures across the ISZ and TSZ. In vertical cross section A-a across the TSZ between northern Germany and southern Sweden, we find a fast anomaly dipping towards the southwest down to depths of nearly 200 km (see Figure 3b). The location of this fast anomaly coincides with the Elbe lineament on the surface [*Shomali et al.*, 2002, 2006]. In agreement with body-wave tomographic results based on TOR array data [*Shomali et al.*, 2002, 2006], the lithosphere of EU_{30} is relatively thin (~100 km) beneath northern Germany. Within a very short horizontal distance, the lithosphere becomes much thicker (nearly 200 km–300 km) beneath southern Sweden. In the image from *Shomali et al.* [2002, 2006], the fast wavespeed body is detached from the surface. However, in our image, the SW dipping fast anomaly is continuous from the surface down to 200 km depth. Furthermore, our image

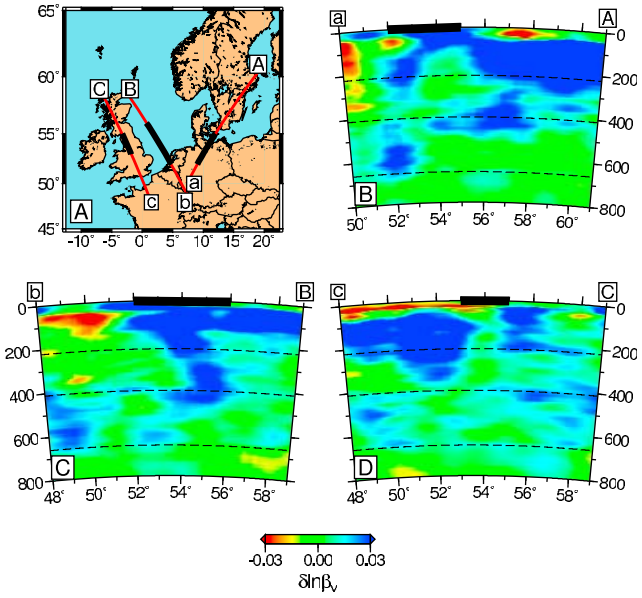

Figure 3. Relative perturbations in the wavespeed of vertically propagating and horizontally polarized shear waves, $\delta \ln \beta_v$, in three vertical cross sections across the ISZ and the TSZ. (a) Map locations of three vertical cross sections; black bars denote locations of interest in Figures 3b–3d. (b) Relative wavespeed perturbations in vertical cross section a-A. (c) Relative wavespeed perturbations in vertical cross section b-B. (d) Relative wavespeed perturbations in vertical cross section c-C.

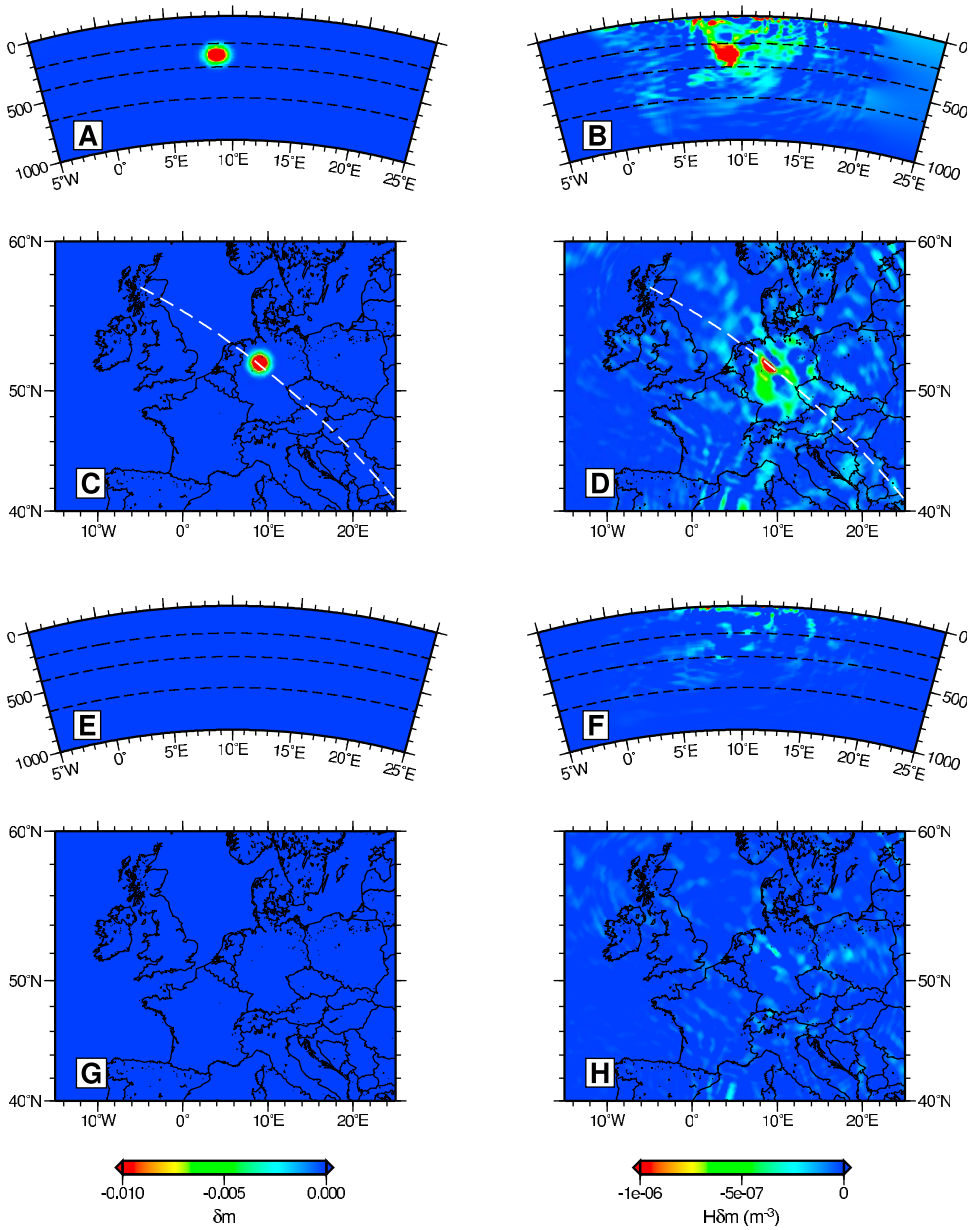

Figure 4. Resolution test for image quality across the TSZ. (a and c) Vertical and horizontal cross sections through a Gaussian perturbation in β_v with respect to model EU_{30}. The dashed white line in Figure 4c indicates the location of vertical cross section in Figure 4a. (b and d) Vertical and horizontal cross sections of the point-spread function for β_v. (e and g) Vertical and horizontal cross sections for perturbations in β_h, which are absent, that is, we are only perturbing β_v. (f and h) Point-spread functions for β_h, illustrating limited tradeoff between β_v and β_h.

for the A-a cross section is consistent with tomographic results from [*Amaru*, 2007]. At ~52°N, the fast anomaly within the transition zone beneath northern Germany may be a detachment from the fast lithospheric anomaly at 200 km depth. From approximately 250 km to 450 km, between 54°N and 58°N, there is an interesting fast anomaly laying flat at the 410 km discontinuity, which may be delaminated lithosphere beneath the thick and old Baltic Shield.

[11] In vertical cross section B-b across the ISZ beneath the southern North Sea, we observe a prominent fast anomaly dipping towards the northwest down to nearly 400 km depth (see Figure 3c). Although the location of this anomaly is a little to the southeast of the geologically speculated location of the ISZ, the dip direction of the fast anomaly agrees with such speculations. In addition, the direction of dip of the fast anomaly in EU_{30} is similar to the orientation of crustal reflectors imaged based on 2D active source experiments [*Klemperer and Matthews*, 1987; *Abramovitz et al.*, 1999]. Beneath the northern part of cross section B-b, EU_{30} contains a nearly 120 km thick lithosphere. The slow anomaly in the southern part of the cross section is correlated to the Rhine Graben in western Germany and Netherlands.

[12] In vertical cross section C-c across the central British Isles, we find a "gap" in lithosphere between the northern and southern British Isles (see Figure 3d). The location of this "gap" coincides with the geological exposure of the ISZ in the British Isles. The lithosphere of southern England is

relatively thick, nearly 200–300 km. The thickest part extends down to more than 300 km depth, for instance between 51°N and 53°N. Previous wide-angle reflection studies found a significant contrast in crustal structure across the ISZ [*Abramovitz et al.*, 1998, 1999; *Abramovitz and Thybo*, 2000]. Based on our image, the structural contrast between Laurentia and Eastern Avalonia extends through the crust and into the lithosphere. It is interesting to note that such a contrast can, apparently, be preserved within the upper mantle over hundreds of millions of years.

[13] In order to assess the quality of these images, we perform a "point-spread function" test [*Fichtner and Trampert*, 2011, 2012]. A Gaussian anomaly with a half width of 60 km and a 2% shear wavespeed reduction is used to perturb model EU_{30} beneath the TSZ, as illustrated in Figure 4. Although there is some smearing across the TSZ, its main features are preserved and well-localized. By comparing the results for vertically and horizontally propagating and horizontally polarized shear wavespeeds, β_v and β_h, respectively, we are confident that there is limited tradeoff between these two parameters. This resolution test confirms the quality of the images used in our paleotectonic interpretation of model EU_{30}.

4. Discussion and Conclusion

[14] It is fascinating that we are still able to observe several prominent upper mantle wavespeed anomalies —related to the closure of the Iapetus Ocean and the Tornquist Sea— despite the fact that after the Caledonian orogeny the area was affected by a host of subsequent tectonic events, such as the Variscan and Alpine orogenies. Compared to previous seismic studies based on wide-angle active source experiments, model EU_{30} enables us to explore much deeper structures beneath the ISZ and TSZ. Furthermore, seismic studies based on dense local arrays, such as the TOR array [*Shomali et al.*, 2002, 2006], are unable to constrain the 3D geometry of these two suture zones, and the current resolution of global tomography is insufficiently detailed.

[15] By exploring European crust and upper mantle model EU_{30} beneath northwestern Europe, we observe two fast anomalies across the ISZ and TSZ. One dips towards the NW and extends down to nearly 400 km beneath the North Sea, and the other dips towards the SW and extends down to nearly 200 km beneath the TSZ. These characteristics agree with geological speculation with regards to the closings of the Iapetus Ocean and the Tornquist Sea. A resolution test across the TSZ confirms the image quality of this feature. In addition, across the ISZ beneath the central British Isles, we find a "gap" between the lithospheres of Laurentia and Eastern Avalonia, which is consistent with a previously observed contrast in crustal structure across this suture zone. Understanding how seismic features capturing the closure of the Iapetus Ocean and Tornquist Sea are preserved within the upper mantle for such a long time requires detailed future geodynamic and tectonic modeling.

[16] **Acknowledgments.** This research was supported by the US National Science Foundation under grants EAR-1112906 and OCI-1063057. We thank Jerry X. Mitrovica and an anonymous reviewer for constructive reviews which helped to improve an earlier version of the paper.

[17] The Editor thanks the anonymous reviewers for assisting in the evaluation of this paper.

References

Abramovitz, T., and H. Thybo (2000), Seismic images of Caledonian, lithosphere-scale collision structure in the southeastern North Sea along MONA LISA Profile 2, *Tectonophysics*, *317*, 27–54.

Abramovitz, T., H. Thybo, and M. L. W. Group (1998), Seismic structure across the Caledonian Deformation Front along the MONA LISA profile 1 in the southeastern North Sea, *Tectonophysics*, *1998*, 153–176.

Abramovitz, T., M. Landes, H. Thybo, A. Jacob, and C. Prodehl (1999), Crustal velocity structure across the Tornquist and Iapetus Suture Zones-a comparison based on MONA LISA and VARNET data, *Tectonophysics*, *314*, 69–82.

Amaru, M. (2007), Global travel time tomography with 3-D reference models, PhD thesis, Utrecht Univ., Utrecht, Netherlands.

Arlitt, R., E. Kissling, J. Ansorge, and T. W. Group (1999), Three-dimensional crustal structure beneath the TRO array and effects on teleseismic wavefronts, *Tectonophysics*, *314*, 309–319.

Artemieva, I., H. Thybo, and M. Kaban (2006), Deep Europe today: Geophysical synthesis of the upper mantle structure and lithospheric processes over 3.5 Ga, in *European Lithosphere Dynamics*, edited by D. G. Gee and R. A. Stephenson, *Mem. Geol. Soc.*, *32*, 11–41.

Bijwaard, H., and W. Spakman (2000), Non-linear global p-wave tomography by iterated linearized inversion, *Geophys. J. Int.*, *141*, 71–82.

Bott, M., R. Long, A. Green, A. Lewis, M. Sinha, and D. Stevenson (1985), Crustal structure south of the Iapetus suture beneath northern England, *Nature*, *314*, 724–727.

Cocks, L., and R. Fortey (1982), Faunal evidence for oceanic sepeartions in the Palaeozoic of Britain, *J. Geol. Soc.*, *139*, 465–478.

Dahlen, F. A., G. Nolet, and S.-H. Hung (2000), Fréchet kernels for finite-frequency traveltime—I. Theory, *Geophys. J. Int.*, *141*, 157–174.

Fichtner, A., and J. Trampert (2011), Hessian kernels of seismic data functionals base upon adjoint techniques, *Geophys. J. Int.*, *185*, 775–798.

Fichtner, A., and J. Trampert (2012), Resolution analysis in full waveform inversion, *Geophys. J. Int.*, *187*, 1604–1624.

Fichtner, A., B. Kennett, H. Igel, and H. Bunge (2009), Full seismic waveform tomography for upper-mantle structure in the Australasian region using adjoint methods, *Geophys. J. Int.*, *179*, 1703–1725.

Fichtner, A., B. Kennett, H. Igel, and H. Bunge (2010), Full waveform tomography for radially anisotropic structure: New insights into present and past states of the Australasian upper mantle, *Earth Planet. Sci. Lett.*, *290*, 270–280.

Fletcher, R., and C. Reeves (1964), Function minimization by conjugate gradients, *Comput. J.*, *7*, 149–154.

Gregersen, S., P. Voss, and T. W. Group (2002), Summary of project TOR: Delineation of a stepwise, sharp, deep lithosphere transition across Germany-Denmark-Sweden, *Tectonophysics*, *360*, 61–73.

Heeremans, M., B. Larsen, and H. Stel (1996), Paleostress reconstruction from kinematic indicators in the Oslo Graben, southern Norway: New constrains on the model of rifing, *Tectonophysics*, *266*, 55–79.

Hung, S.-H., F. A. Dahlen, and G. Nolet (2000), Fréchet kernels for finite-frequency traveltime—II. Examples, *Geophys. J. Int.*, *141*, 175–203.

Klemperer, S., and D. Matthews (1987), Iapetus suture located beneath the North Sea by BIRPS deep seismic reflection profiling, *Geology*, *15*, 195–198.

Komatitsch, D., and J. Tromp (1999), Introduction to the spectral-element method for 3-D seismic wave propagation, *Geophys. J. Int.*, *139*, 806–822.

Komatitsch, D., and J. Tromp (2002a), Spectral-element simulations of global seismic wave propagation-I. Validataion, *Geophys. J. Int.*, *149*, 390–412.

Komatitsch, D., and J. Tromp (2002b), Spectral-element simulations of global seismic wave propagation—II. Three-dimensional models, oceans, rotation and self-gravitation, *Geophys. J. Int.*, *150*, 308–318.

Kustowski, B., G. Ekström, and A. M. Dziewoński (2008), Anisotropic shear-wave velocity structure of the Earth's mantle: A global model, *J. Geophys. Res.*, *113*, B06306, doi:10.1029/2007JB005169.

Landes, M., C. Prodehl, F. Hauser, A. Jacob, and N. Vermeulen (2000), VARNET-96: Influence of the Variscan and Caledonian orogenies on crustal stucture in SW Ireland, *Geophys. J. Int.*, *140*, 660–676.

Lebedev, S., and R. van der Hilst (2008), Global upper-mantle tomography with the automated multimode inversion of surface and S-wave forms, *Geophys. J. Int.*, *173*, 505–518.

Liu, Q., and J. Tromp (2006), Finite-frequency sensitivity kernels based upon adjoint methods, *Bull. Seismol. Soc. Am.*, *96*, 2383–2397.

Liu, Q., and J. Tromp (2008), Finite-frequency sensitivity kernels for global seismic wave propagation based upon adjoint methods, *Geophys. J. Int.*, *174*, 265–286.

Lyngsie, S., and H. Thybo (2007), A new tectonic model from the Laurentia-Avalonia-Baltica structures in the North Sea: A case study along MONA LISA profile 3, *Tectonophysics*, *429*, 201–227.

Lyngsie, S., H. Thybo, and T. Rasmussen (2006), Regional geological and tectonic structures of the North Sea area from potential field modelling, *Tectonophysics*, *413*, 147–170.

Medhus, A., N. Balling, B. Jacobsen, C. Weidle, R. England, R. Kind, H. Thybo, and P. Voss (2012), Upper-mantle structure beneath the Southern Scandes Mountains and the Northern Tornquist Zone revealed by P-wave traveltime tomography, *Geophys. J. Int.*, *189*, 1315–1334.

Piromallo, C., and A. Morelli (2003), P wave tomography of the mantle under the Alpine-Mediterranean area, *J. Geophys. Res.*, *108*(B2), 2065, doi:10.1029/2002JB001757.

Shomali, Z., R. Roberts, and the TOR Working Group (2002), Non-linear body wave teleseismic tomography along the tor array, *Geophys. J. Int.*, *148*, 562–574.

Shomali, Z., R. Roberts, L. Pedersen, and the TOR Working Group (2006), Lithospheric structure of the Torquist Zone revealed by nonlinear P and S teleseismic tomography along the TOR array, *Tectonophysics*, *416*, 133–149.

Tape, C., Q. Liu, and J. Tromp (2007), Finite-frequency tomography using adjoint methods—Methodology and examples using membrane surface waves, *Geophys. J. Int.*, *168*, 1105–1129.

Tape, C., Q. Liu, A. Maggi, and J. Tromp (2009), Adjoint tomography of the Southern California crust, *Science*, *325*, 988–992.

Tape, C., Q. Liu, A. Maggi, and J. Tromp (2010), Seismic tomography of the Southern California crust based on spectral-element and adjoint methods, *Geophys. J. Int.*, *180*, 433–462.

Tarantola, A. (1984), Inversion of seismic reflection data in the acoustic approximation, *Geophysics*, *49*, 1259–1266.

Tromp, J., C. Tape, and Q. Y. Liu (2005), Seismic tomography, adjoint methods, time reversal and banana-doughnut kernels, *Geophys. J. Int.*, *160*, 195–216.

Zhu, H., E. Bozdag, D. Peter, and J. Tromp (2012), Structure of the European upper mantle revealed by adjoint tomography, *Nat. Geosci.*, *5*, 493–498.

Zielhuis, A., and G. Nolet (1994a), Deep seismic expression of an ancient plate boundary in Europe, *Science*, *265*, 79–81.

Zielhuis, A., and G. Nolet (1994b), Shear-wave velocity variations in the upper mantle beneath central Europe, *Geophys. J. Int.*, *117*, 695–715.